

Heterogeneous and Homogeneous Electron Transfers to Aromatic Halides. An Electrochemical Redox Catalysis Study in the Halobenzene and Halopyridine Series

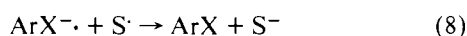
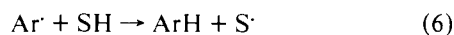
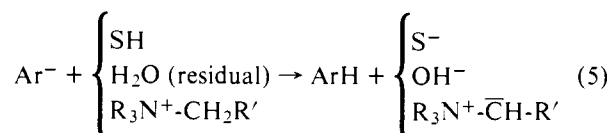
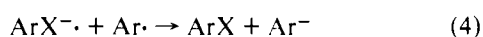
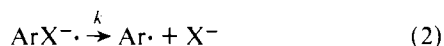
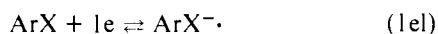
Claude P. Andrieux, Claude Blocman, Jean-Michel Dumas-Bouchiat, and Jean-Michel Saveant*

Contribution from the Laboratoire d'Electrochimie de l'Universit  de Paris VII, 2 Place Jussieu, 75221, Paris Cedex 05, France. Received October 18, 1978

Abstract: Halobenzenes and halopyridines undergo a two-electron irreversible reductive cleavage. It involves fast decomposition of the assumed anion radical intermediate, $\text{ArX}^{\cdot-}$ ($k_{1st\ order} \gg 10^4\ \text{s}^{-1}$), and transient formation of a neutral radical, Ar, easier to reduce than the starting molecule. With the exception of PhI, the electrochemical reaction is under the kinetic control of the initial electron transfer step. Standard application of the electrochemical techniques provides the transfer coefficients and the forward electron transfer rate constants but no information about the standard potentials and the standard rate constants. The latter quantities can be determined through the kinetic analysis of homogeneous redox catalysis of the electrochemical reduction. The following points are discussed: activation vs. diffusion control of the homogeneous electron transfer; existence of the anion radical as an actual reaction intermediate vs. simultaneous electron transfer and breaking of the carbon-halogen bond; correlation between homogeneous and heterogeneous electron transfers; determination of the standard potentials and the standard rate constants; relationships between structure and electron transfer thermodynamics and kinetics. The remarkable slowness of the electron transfer as compared to aromatic and heteroaromatic compounds of similar molecular size implies, besides solvent reorganization, a significant internal reorganization due to stretching of the carbon-halogen bond when passing from the starting molecule to the anion radical.

Introduction

The electrochemical reduction of aromatic halides in organic nonaqueous solvents (see ref 1 and references cited therein) generally involves, in the cases of Cl, Br, and I, the cleavage of the carbon-halogen bond of the initially generated anion radical.



The neutral radical thus formed may then undergo an electrode (3) or a solution reduction (4) leading, after protonation by the solvent, the residual water, or the quaternary ammonium cation of the supporting electrolyte (5), to an overall hydrogenolysis of the carbon-halogen bond. Ar \cdot may also abstract a hydrogen atom from the solvent (6), the solvent radical thus formed being further reduced to the solvent conjugated base at the electrode (7) or in the solution (8). In such conditions, the main reduction process will then appear as a two-electron irreversible wave provided that the lifetime of the $\text{ArX}^{\cdot-}$ anion radical is short within the time scale of the experiment. The yield of ArH upon electrolysis at the potential of this wave will then be 100%. This is what is observed in a number of cases, e.g., with chloro- and bromobenzene,³ chlorobiphenyl,⁴ and 1-chloro-, bromo-, and iodobenzonitriles.⁶ A second wave is observed when ArH is reducible before the background discharge, its reversibility depending upon the stability of the $\text{ArH}^{\cdot-}$ anion radical.

In some cases, however (see ref 1 and references cited therein), the apparent number of faradays per mole at the first wave is less than 2 and the yield in ArH significantly less than 100%. This phenomenon has been analyzed in detail in the case of 4-bromobenzophenone and has been shown to be caused by an $\text{S}_{\text{NR}}1$ substitution of the halogen by the solvent conjugated base S^- .^{1,2} The substitution products give rise themselves to reduction waves that cannot practically be distinguished from that of ArH. That such a process occurs to a much lesser extent in the present ArX series can be explained in this context by the weaker electrophilic character of the Ar \cdot radical. It could, however, be more effective at potentials located at the foot of the second wave as revealed by the frequent occurrence of a current dip in this region.⁷ Such dips are indeed observed when the electron-induced substitution is carried out with purposely added nucleophiles² and can be interpreted as an acceleration of the substitution process in this potential region.⁷

A detailed discussion of these phenomena is beyond the scope of the present paper and will be the object of forthcoming publications. We will here focus our attention upon halo compounds that give rise to a two-electron process with 100% ArH yield at the first wave, the reduction mechanism of which can be pictured by the above scheme (reactions 1-8) without further interference of the solvent conjugated base.

When reaction 2 is fast, i.e., for rate constants larger than 10^4 - $10^5\ \text{s}^{-1}$, no chemical reversibility can be detected using the electrochemical kinetic techniques even at the lowest extremity of their time scale (e.g., cyclic voltammetry with sweep rates in the kilovolt per second range). With the exception of compounds bearing strong electron-withdrawing groups, such as COR and NO_2 , this is a very common situation among the chloro, bromo, and iodo aromatics. The kinetic control of the reduction process is then by the initial electron transfer (1) and the cleavage reaction (2). If the initial electron transfer is slow and/or the cleavage reaction is fast the reduction process tends to be kinetically controlled by the electron transfer.⁸ When such a situation prevails the standard application of the usual electrochemical techniques gives no information not only about the lifetime of $\text{ArX}^{\cdot-}$ but also about the standard potential, E^\ominus , and the electrochemical standard rate constant, $k_{\text{S}^{\ominus 1}}$, of the $\text{ArX}/\text{ArX}^{\cdot-}$ couple. The only available data are then the

transfer coefficient α and the electrochemical forward rate constant:

$$k_1^{e1} = k_S^{e1} \exp(\alpha FE^0/RT)$$

of the electron transfer. In other words, the kinetics and the thermodynamics of the electrode electron transfer cannot be characterized separately.

It has been recently shown⁹ that the kinetic analysis of homogeneous redox catalysis¹⁰ of such electrochemical reactions by a series of reversible redox couples may provide a much more complete characterization of the electron-transfer process allowing the determination of the standard heterogeneous rate constant. It provides in addition the value of the standard rate constant of the homogeneous electron transfer.

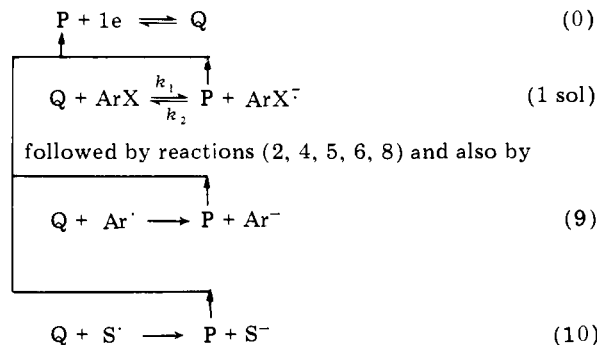
The method was illustrated by the experimental study of the reduction of chlorobenzene using classical polarography.⁹

One purpose of the present paper is to describe the application of the method to a series of aromatic halides using cyclic voltammetry for which the theory of homogeneous catalysis has been recently worked out.¹¹ Cyclic voltammetry indeed leads to a better accuracy than polarography and to an extension of the potential range in which the electron-transfer kinetics can be determined. Time needed to record a cyclic voltammogram is much shorter than for a polarogram. This leads to a very significant time saving since a detailed redox catalysis study requires a large number of experiments involving a series of redox couples.

The compounds selected for this study—chloro-, bromo-, and iodobenzene and 2- and 3-chloro- and -bromopyridine—fall, with the exception of iodobenzene, in the category defined above, i.e., give rise to an irreversible 2e reduction kinetically controlled by the forward electron transfer at the electrode as well as in the solution. The thermodynamic and kinetic data obtained from the redox catalysis study of these compounds will then serve to discuss the following points: activation vs. diffusion control of the homogeneous electron transfer; existence of the anion radical as an actual reaction intermediate vs. simultaneous electron transfer and breaking of the carbon-halogen bond which is a problem of general interest for both aliphatic and aromatic halo compounds (see, e.g., ref 12-14); correlation between homogeneous and heterogeneous electron-transfer kinetics; relationships between structure and electron-transfer thermodynamics and kinetics.

Redox Catalysis as a Method for Determining Standard Potentials and Standard Electron Transfer Rate Constants

The method consists in introducing into the solution the oxidized form P of a chemically and electrochemically reversible couple P/Q, the redox catalyst, the standard potential of which, E^0_{PQ} , is positive to the reduction potential ArX. The reduced form Q is then generated at the electrode and transfers an electron to the substrate ArX within the electrode diffusion layer giving rise to the following reaction sequence:

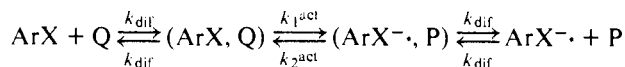


P is regenerated through reactions (1 sol), (9), and (10) resulting in an enhancement of its reduction current as com-

pared to that observed in absence of substrate. This "catalytic" effect is only a function of k_1 in the case where the forward homogeneous electron transfer is the rate-determining step. It can therefore be used to determine k_1 according to an appropriate treatment of the kinetics of this phenomenon.⁹ The experiment and treatment of data are then repeated with other catalyst couples so as to explore the largest possible range of standard potentials.

The kinetics of the cross electron exchange between the ArX/ArX⁻ and P/Q couples, as reflected by the values of k_1 and k_2 , is under the control of both activation and diffusion factors and is a function of the intrinsic characteristics of the electron transfer to each couple.¹⁵ However, when using as catalysts aromatic or heteroaromatic molecules, both the diffusion coefficient and the isotopic activation free energy of the catalyst can be considered as approximately constant in the series.¹⁶ It is also noted that the isotopic free energies of activation are small,¹⁶ which reinforces the validity of the approximation. In this context, the variations of k_1 from one catalyst to the other reflects how the intrinsic kinetics of electron transfer in the ArX/ArX⁻ varies with potential.

In order to describe the relative interference of activation and diffusion factors, let us consider reaction (1 sol) as composed of three successive steps:



(ArX, Q) and (ArX⁻, P) represent the reactants in their reaction sites, whereas ArX + Q and ArX⁻ + P represent the reactants beyond the average diffusion distance. k_{dif} is the diffusion-limited rate constant, and k_1^{act} and k_2^{act} are the activation-controlled rate constants. Writing the stationary-state assumption for both (ArX, Q) and (ArX⁻, P) one readily obtains the expression of k_1 as

$$(1/k_1) = (1/k_1^{\text{act}}) + (1/k_{\text{dif}})[1 + \exp(F/RT)(E^0_{PQ} - E^0)] \quad (11)$$

with

$$\log k_1^{\text{act}} = \log k_S^{\text{sol}} - \alpha^{\text{sol}}(E^0_{PQ} - E^0)/0.058 \quad (\text{at } 22^\circ\text{C}) \quad (12)$$

where α^{sol} and k_S^{sol} are the transfer coefficient and the standard rate constant of the homogeneous electron transfer to the ArX/ArX⁻ couple. α^{sol} is close to 0.5 when the potential is not too far from the E^0 . According to the magnitude of $E^0_{PQ} - E^0$ two zones of diffusion control with 0 and $-1/58$ mV slopes, respectively, and an intermediate zone of activation control with a $-1/116$ mV slope are obtained on the $\log k_1 - E^0_{PQ}$ plots as shown in Figure 1. The extension of the activation zone is larger the lower k_S^{sol} .

The possibility of determining E^0 is based on the experimental observation of the diffusion zone at $E^0_{PQ} > E^0$: E^0 is then obtained by extrapolation of the corresponding straight line up to the value of the diffusion-limited rate constant. The existence of this diffusion-controlled zone is not significantly affected by reaction 2 as long as it is not so fast as to occur within the average diffusion distance. The latter quantity being on the order of molecular sizes, this condition will be fulfilled as long as k is smaller than about 10^{10} s^{-1} . It is noted incidentally that beyond this limit the very existence of the ArX⁻ anion radical becomes ambiguous.

The homogeneous electron transfer process can be considered as an electrolysis with an extremely small diffusion layer thickness, on the order of a few ångströms, as opposed to electrolysis in the context of the usual electrochemical techniques where the diffusion layer thickness is at best 1000 times larger. In electrochemical conditions reaction 2 occurs within a small portion of the diffusion layer whereas in homogeneous

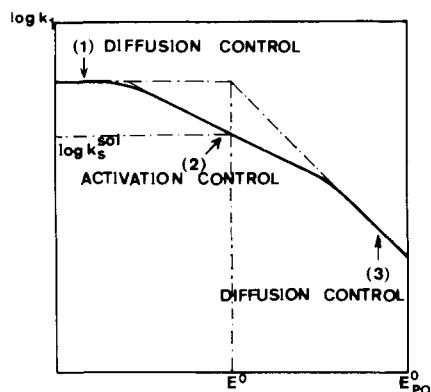


Figure 1. Predicted variations of the homogeneous forward electron transfer rate constant with potential showing activation and diffusion control. (1) Diffusion control: $\log k_1 = \log k_{\text{dir}}$. (2) Activation control: $\log k_1 = \log k_{\text{S}}^{\text{sol}} - \alpha^{\text{sol}}(E_{\text{PQ}}^0 - E^0)/0.058$. (3) Diffusion control: $\log k_1 = \log k_{\text{dir}} - (E_{\text{PQ}}^0 - E^0)/0.058$.

conditions it occurs outside the diffusion layer. These are fundamental reasons why in the present case quantities such as E^0 are inaccessible through electrochemical techniques while they can be obtained through redox catalysis which thus amounts to be a "molecular sized electrode electrolysis."

On the other hand, reaction 2 has been assumed to be fast enough so as the forward reaction (1 sol) is the rate-determining step. The condition to be fulfilled then is $k > k_2 C_{\text{PQ}}^0$. (C_{PQ}^0 is the bulk concentration of the catalyst.) If k_2 is at the diffusion limit and with standard experimental condition this amounts to $k > 10^6 - 10^7 \text{ s}^{-1}$. This point can anyway be checked experimentally since the catalytic increase of the current has a characteristic dependence upon C_{PQ}^0 when (1 sol) is the rate-determining step whereas there is no concentration dependence when (2) is the rate-determining step. It is indeed clear that the overall process is second order toward Q in the former case and first order in the latter.

Once E^0 is determined using the above procedure, the standard rate constant of the homogeneous electron transfer $k_{\text{S}}^{\text{sol}}$ is obtained as shown in Figure 1. This requires the activation control domain not to be too small in order to be able to locate the straight line with the $-1/116 \text{ mV}$ slope.

The activation free energy of the cross exchange reaction is given by

$$\Delta G_{\text{sol}}^*/F = 0.058 \log (Z^{\text{sol}}/k_{\text{S}}^{\text{sol}}) \quad (13)$$

(Z^{sol} : collision frequency in the solution) and the intrinsic kinetic characteristics of the homogeneous electron transfer to ArX can then be obtained from¹⁵

$$\Delta G_{\text{sol}}^* = (\Delta G_{\text{ArX}}^*_{\text{iso}} + \Delta G_{\text{P}}^*_{\text{iso}})/2 \quad (14)$$

under the form of the activation free energy of the isotopic transfer to ArX if the corresponding quantity is known for the catalysts. When employing aromatic or heteroaromatic molecules as catalysts an average value¹⁶

$$\Delta G_{\text{P}}^*_{\text{iso}}/F = 0.159 \text{ V}$$

can be used with a good approximation.

Knowing E^0 , the heterogeneous electron transfer kinetics can also be characterized. Using, e.g., cyclic voltammetry, the electrochemical transfer coefficient, α , and standard rate constant, k_{S}^{el} , can be derived from the measurement of the peak potential as a function of sweep rate v :¹⁷

$$(\partial E_{\text{p}}/\partial \log v) = -0.058/\alpha \text{ V} \quad (15)$$

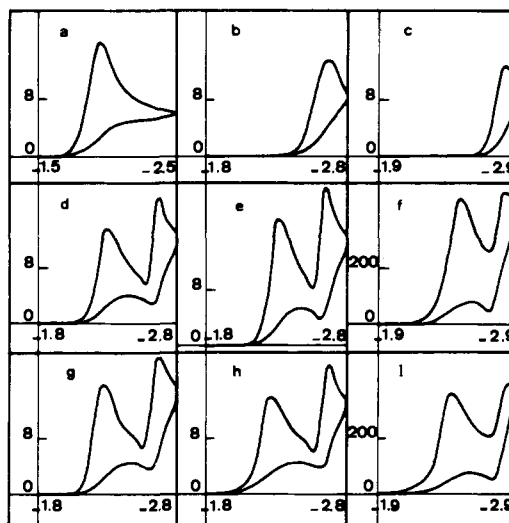


Figure 2. Cyclic voltammetry of halobenzenes and halopyridines: (a) PhI, (b) PhBr, (c) PhCl, (d) 3-pyCl, (e) 2-pyCl, (g) 2-pyBr (h) 3-pyBr at 0.33 V s^{-1} ; (f) 3-pyCl, (i) 2-pyBr at 330 V s^{-1} . Substrate concentration $2 \times 10^{-3} \text{ M L}^{-1}$. Vertical scale: μA . Horizontal scale: V vs. SCE.

and

$$E_{\text{p}} = E^0 + (0.058/\alpha) \log k_{\text{S}}^{\text{el,ap}} - (1/\alpha)[0.067 + 0.029 \log \alpha v D]$$

at 22°C .

$k_{\text{S}}^{\text{el,ap}}$ is the electrochemical apparent standard rate constant, i.e., uncorrected from double-layer effects. The standard rate constant is then obtained through the Frumkin correction:

$$\log k_{\text{S}}^{\text{el}} = \log k_{\text{S}}^{\text{el,ap}} - (\alpha\phi_2/0.058) \quad (16)$$

where ϕ_2 is the potential difference between the outer Helmholtz plane and the solution. The activation free energy of the heterogeneous electron transfer is finally given by

$$\Delta G_{\text{el}}^*/F = 0.058 \log (Z^{\text{el}}/k_{\text{S}}^{\text{el}}) \quad (17)$$

(Z^{el} : heterogeneous collision frequency).

Experimental Section

Electrochemical Instrumentation and Procedures. The experiments were carried out in DMF with $0.1 \text{ M Bu}_4\text{Nl}$ as supporting electrolyte. The temperature was 22°C . The working electrode used in cyclic voltammetry was a mercury drop hanging on a gold disk of about 0.8 mm^2 surface area. The reference electrode was an aqueous saturated calomel electrode. The solution resistance was compensated using a positive feedback device down to a residual value on the order of 10Ω . The procedure for extracting the values of k_1 for each catalyst couple was similar to that used in polarography⁹ involving the determination of the catalytic efficiency for a series of values of the substrate/catalyst concentration ratio in each case. Working curves corresponding to cyclic voltammetry¹¹ were used for deriving k_1 from the catalytic efficiency. When possible, i.e., for not too slow catalytic processes, several sweep rates were employed in order to obtain a better accuracy than in polarography. For high-efficiency catalysis corresponding to the wave of the catalyst being close to the wave of the substrate, sweep rates up to 1000 V s^{-1} were used, allowing the investigation of a more extended potential range than in polarography. A more detailed description of the procedure and discussion of these points is given elsewhere.¹¹

Chemicals. The aromatic halides were obtained from commercial sources (chloro-, bromo-, and iodobenzene, Prolabo; 2- and 3-chloro- and -bromopyridine, EGA Chemie) and were used as received.

Results

Electrochemical Behavior. Figure 2 shows the cyclic voltammograms obtained with the seven aromatic halides at

Table I. Electrochemical Characteristics of Halobenzenes and Halopyridines^a

	PhCl	PhBr	PhI	3-pyCl	2-pyCl	3-pyBr	2-pyBr
$i_p v^{-1/2}$, $\mu\text{A V}^{-1/2} \text{s}^{1/2}$	23 ± 2^b	22 ± 2	26 ± 2	23 ± 2	28 ± 2	22 ± 2	25 ± 2
av between 0.33 and 100 V s^{-1}							
$-\partial E_p / \partial \log v$, mV/unit, from 0.1 to 100 V s^{-1}	55 ± 3^b	64 ± 2	48 ± 2	56 ± 2	57 ± 2	60 ± 2	58 ± 2
ΔE_p , mV (av), between 10 and 100 V s^{-1}	85 ± 5	95 ± 5	75 ± 5	84 ± 5	84 ± 5	90 ± 5	88 ± 5
α (av) (from $-\partial E_p / \partial \log v$)	0.53 ± 0.03	0.45 ± 0.02	0.60 ± 0.02	0.52 ± 0.02	0.51 ± 0.02	0.48 ± 0.02	0.50 ± 0.02
$k_f^{\text{et,ap}}$	7.5×10^{-27}	2.2×10^{-25}	3.0×10^{-19}	1.5×10^{-22}	8.5×10^{-23}	5.0×10^{-22}	2.8×10^{-22}

^a i_p = peak current; E_p = peak potential; ΔE_p = peak width; v = sweep rate; α = transfer coefficient; $k_f^{\text{et,ap}}$ = apparent forward rate constant of electron transfer. ^b Determined between 0.1 and 2 V s^{-1} only, since for higher sweep rates the wave merges with the discharge current of the supporting electrolyte.

Table II. Redox Catalysis of Bromobenzene Reduction

catalyst	E_{PQ}^0 , V vs. SCE	typical values of γ and v , V s^{-1}		$(i_p)_c / (i_p)_0$	$\log k_1$, $\text{M}^{-1} \text{L s}^{-1}$	av
anthracene	-1.89	20	0.033	1.21	0.4	0.4
		50	0.033	1.46	0.4	
		50	0.33	1.06	0.5	
phenanthridine	-2.00	20	0.33	1.37	1.7	1.8
		50	0.33	2.07	1.9	
		50	3.3	1.10	1.8	
benzo[<i>f</i>]quinoline	-2.08	5	0.33	2.7	3.1	3.1
		20	0.33	5.2	3	
		5	3.3	1.28	3.2	
		50	3.3	2.85	3.1	
		50	33	1.28	3.1	
benzo[<i>h</i>]quinoline	-2.12	5	0.33	2.8	3.1	3.3
		20	0.33	5.8	3.2	
		5	3.3	1.3	3.3	
		20	3.3	2.3	3.3	
		50	33	1.48	3.4	
chrysene	-2.20	1	0.33	1.87	3.6	3.7
		5	0.33	5.2	3.8	
		2	3.3	1.4	3.7	
		10	3.3	2.5	3.6	
		20	33	1.3	3.6	
		50	33	1.9	3.7	
benzonitrile	-2.24	2	0.33	3.90	4.2	4.3
		10	0.33	11.4	4.3	
		1	3.3	1.6	4.3	
		5	3.3	3.8	4.4	
		20	33	2.8	4.4	
<i>m</i> -toluonitrile	-2.27	1	3.3	1.75	4.4	4.5
		5	3.3	4.0	4.5	
		20	3.3	9.4	4.6	
		10	33	2.1	4.5	
<i>p</i> -toluonitrile	-2.34	0.5	3.3	1.8	5.0	5.2
		5	3.3	8	5.4	
		2	33	2	5.2	
		5	33	3.2	5.2	
phenanthrene	-2.41	2	10	3.8	5.6	5.6
		5	10	6.7	5.6	
		1	100	1.4	5.5	
		2	100	1.8	5.6	

moderate sweep rates. The cyclic voltammograms remain irreversible up to 2000 V s^{-1} , showing that, if the anion radical is actually the first reaction intermediate, its decomposition is fast (lifetime smaller than 10^{-4} s). With the halopyridines the first irreversible wave is followed by a wave located at the same potential as that obtained with pyridine itself, showing the formation of pyridine by reductive cleavage of the halogen at the first wave.

The cathodic peak current is proportional to the square root of sweep rate within experimental uncertainty (Table I). The value of $i_p v^{-1/2}$ is almost the same for the seven compounds.

The slight differences observed passing from one compound to the other are more likely to be due to some irreproducibility in electrode surface area than to actual variations in the apparent number of electrons. Since it is known that chloro- and bromobenzene³ are reduced along a two-electron process leading quantitatively to ArH, it can be concluded that this is also the case with the other compounds, the difference in diffusion coefficients being negligible. To further check this point, coulometric experiments were carried out in the case of iodobenzene and 2-chloro- and 2-bromopyridine; they all gave an apparent number of electrons between 1.8 and 2 and a quan-

Table III. Redox Catalysis of Chlorobenzene Reduction

catalyst	E°_{PQ} , V vs. SCE	typical values of γ and v , $V s^{-1}$		$(i_p)_c/(i_p)_0$	$\log k_1$, $M^{-1} L s^{-1}$	av
benzonitrile	-2.24	20	0.033	1.25	0.5	0.5
		50	0.033	1.50	0.5	
		50	0.33	1.06	0.5	
phenanthrene	-2.41	2	0.033	3.2	2.8	2.9
		10	0.033	8.0	2.8	
		2	0.33	1.45	2.8	
		20	0.33	4.9	2.8	
		10	3.3	1.3	2.9	
		50	3.3	2.8	2.9	
diphenyl	-2.54	2	0.033	5.2	4.1	4.3
		2	0.33	4.4	4.4	
		10	0.33	14.4	4.5	
		1	3.3	1.65	4.3	
		5	3.3	4.1	4.5	
		5	33	1.50	4.5	

titative yield of pyridine as checked by cyclic voltammetry of the electrolyzed solution.

A separate cyclic voltammetric study of pyridine in the same medium shows that a two-electron irreversible behavior is observed at low sweep rates. Chemical reversibility appears upon raising the sweep rate and is practically complete at 2000 $V s^{-1}$, resulting then in a one-electron quasi-reversible behavior due to charge-transfer slowness. The second wave of halopyridines also shows increased reversibility and tendency toward one-electron behavior upon raising the sweep rate. This is apparently obtained somewhat more easily than in the case of pyridine itself. This is in fact the anodic counterpart of the dip observed on the cathodic trace at the foot of the second wave. The dip is more apparent in polarography than in cyclic voltammetry and its magnitude decreases upon raising the sweep rate. This is to be related to the interference of substitution by S^- in the framework of an ECE mechanism as discussed in the Introduction. The fact that this phenomenon is more apparent than in the case of, e.g., halonaphthalenes^{1,2} indicates that the electrophilic character of the $Ar\cdot$ radical is enhanced by the presence of the ring nitrogen. Pyridine may indeed be considered as the vinylog of an imine which points to the possibility of localizing a second electron pair and a negative charge on the nitrogen.

All these observations are consistent with a two-electron reductive cleavage of the halogen which can therefore be represented by the reaction sequence (reactions 1e1-8) given above.

The peak potentials were observed to shift linearly with the logarithm of sweep rate in the range 0.1–100 $V s^{-1}$ (Table I). The values of the corresponding slopes $\partial E_p/\partial \log v$ as well as those of the peak width ΔE_p (Table I) show¹⁷ that the electrode reaction is kinetically controlled by the initial charge transfer with the exception of iodobenzene. In the latter case the observed slope is compatible either with a rate-determining charge transfer with a transfer coefficient significantly larger than 0.5 (≈ 0.60) or with a mixed kinetic control by charge transfer and by a follow-up chemical reaction.⁸ In all the other cases the values of the transfer coefficient do not differ significantly from 0.5. That the charge transfer is rate controlling in the case of, e.g., bromobenzene and 2-bromopyridine is confirmed by the negative shift in peak potential when passing from Et_4N^+ to Bu_4N^+ (0.1 M) as supporting cation (120 mV for chlorobenzene and 110 mV for 2-bromopyridine) resulting from a change in the double-layer characteristics.¹⁸ With iodobenzene, the shift is only 40 mV, indicating that mixed charge transfer chemical reaction control is more likely than pure charge transfer control with a large α . The complete ir-

reversibility of the CV wave observed for all compounds prevents the determination of the standard potential and of the standard rate constant. The measurement of the peak potential as a function of sweep rates provides, however, the apparent forward rate constant of electron transfer $k_f^{el,ap}$,¹⁷ the values of which are given in Table I.

Homogeneous Redox Catalysis. In most cases the forward rate constant of electron transfer, k_1 , was determined for the experimental ratio $(i_p)_c/(i_p)_0$ (peak currents of the catalyst wave in the presence and absence of substrate, respectively).¹¹ For very high catalytic efficiencies, this procedure cannot be used safely since $(i_p)_c$ is too close to its limiting value. In such conditions k_1 was derived from the peak potential differences δE_p between the peak potentials for the catalyst wave in presence and in absence of substrate.¹¹ The results are shown in Tables II–VII, which give, for each halo compound with the exception of iodobenzene, the list of the catalysts with their standard potential (E°_{PQ}), typical values of the excess factor (γ : ratio of the concentrations of substrate and catalyst), and sweep rate v with the resulting values of either $(i_p)_c/(i_p)_0$ or δE_p . The k_1 values figured in the last column were obtained as an average corresponding to a larger number of γ and v values than shown in the tables. Figures 3–8 represent the final results as plots of the logarithm of the homogeneous forward rate constant, k_1 , vs. the standard potential of the catalyst couple E°_{PQ} .

In the case of chlorobenzene, the results obtained previously using classical polarography⁹ were used together with those of Table III for the diagram in Figure 4.

Such detailed and systematic analyses were not carried out for iodobenzene since it was not possible in this case to ascertain the nature of the rate-determining steps. An important qualitative observation was, however, made: for a given distance between the catalyst and the substrate waves, catalytic efficiency is always markedly lower for iodobenzene than for either chloro- or bromobenzene.

Discussion

Activation vs. Diffusion Control of the Homogeneous Electron Transfer. The $\log k_1 - E^{\circ}_{PQ}$ plots exhibit two distinct regions. For the most positive potentials, the experimental points are located on a straight line with a slope of about $-1/58$ mV per decade, whereas for the most negative potentials they are situated on a straight line having a slope of about $-1/116$ mV per decade. These two straight lines are joined by a curve in the intermediate potential regions. Actually, these two straight lines are unequally extended depending upon each particular halo compound. The first one just begins to appear with bro-

Table IV. Redox Catalysis of 2-Bromopyridine Reduction

catalyst	E^0_{PQ} , V vs. SCE	typical values of γ and v , V s ⁻¹		$(i_p)_c/(i_p)_0$	$\log k_1$, M ⁻¹ L s ⁻¹	av
naphthonitrile	-1.78	5	0.033	1.30	1.3	1.3
		50	0.033	3.7	1.3	
9,10-diphenyl- anthracene	-1.80	5	0.033	1.40	1.4	1.4
		50	0.033	3.70	1.3	
		20	0.033	1.20	1.4	
anthracene	-1.89	50	0.033	24.2	3.0	3.0
		2	0.33	1.65	2.9	
		20	0.33	5.42	3.1	
		10	3.3	1.34	3.0	
		50	3.3	2.53	2.9	
		50	33	1.20	3.0	
phenanthridine	-2.00	2	0.33	4.2	4.3	4.5
		20	0.33	19.2	4.4	
		1	3.3	2.04	4.6	
		10	3.3	6.5	4.6	
		5	33	1.52	4.5	
benzo[<i>f</i>]quinoline	-2.08	20	0.33	30.8	5.1	5.3
		5	3.3	7.6	5.3	
		50	3.3	39	5.4	
		1	33	1.71	5.4	
		5	33	4.10	5.5	
benzo[<i>h</i>]quinoline	-2.12	20	3.3	31.6	6.1	6.1
		1	33	2.5	6.0	
		5	33	6.8	6.2	
methyl benzoate	-2.17	1	33	2.6	6.1	6.2
		5	33	8.0	6.4	
		0.5	1000	1.19	6.1	
		1	1000	1.43	6.2	
		1	0.033	$\delta E_p = 105$ mV	6.1	
benzonitrile	-2.24	1	0.033	$\delta E_p = 140$ mV	7.3	7.3
		1	0.33	$\delta E_p = 110$ mV	7.3	

Table V. Redox Catalysis of 3-Bromopyridine Reduction

catalyst	E^0_{PQ} , V vs. SCE	typical values of γ and v , V s ⁻¹		$(i_p)_c/(i_p)_0$	$\log k_1$, M ⁻¹ L s ⁻¹	av
naphthonitrile	-1.78	2	0.033	1.3	1.4	1.4
		10	0.033	2.2	1.5	
		20	0.033	2.6	1.4	
9,10-diphenyl- anthracene	-1.80	10	0.033	2.0	1.4	1.4
		20	0.033	2.6	1.4	
		50	0.33	1.7	1.5	
anthracene	-1.89	1	0.033	2.2	2.8	2.9
		2	0.033	3.1	2.8	
		2	0.33	1.6	2.9	
		10	0.33	2.8	2.8	
		20	3.3	1.80	3.0	
phenanthridine	-2.00	2	0.33	4.35	4.4	4.3
		10	0.33	10.5	4.1	
		1	3.3	1.65	4.3	
		10	3.3	5.2	4.4	
		10	33	2.4	4.5	
benzo[<i>h</i>]quinoline	-2.12	10	3.3	19.2	6.1	6.2
		2	33	4.0	6.2	
		20	33	19.0	6.4	
methyl benzoate	-2.17	1	33	2.8	6.4	6.3
		10	33	19.2	6.2	
		0.5	1000	1.1	6.3	

mobenzene and is somewhat more apparent with chlorobenzene; with the bromopyridines the first straight line is dominant. This trend is even more pronounced with the chloropyridines, the second line being almost absent. The comparison

between the six diagrams makes, however, clearer the existence of these two modes of variation of k_1 with E^0_{PQ} noted previously in the case of chlorobenzene.⁹ They correspond, as discussed above, to (1) activation control of the electron

Table VI. Redox Catalysis of 2-Chloropyridine Reduction

catalyst	E^0_{PQ} , V vs. SCE	typical values of γ and v , V s ⁻¹		$(i_p)_c/(i_p)_0$	$\log k_1$, M ⁻¹ L s ⁻¹	av
9,10-diphenyl- anthracene	-1.80	20	0.033	1.06	0.0	0.0
		50	0.033	1.20	0.0	
anthracene	-1.89	10	0.033	1.45	1.1	1.1
		50	0.033	2.90	1.0	
		50	0.33	1.29	1.2	
phenanthridine	-2.00	2	0.33	1.78	3.1	3.1
		20	0.33	5.24	3.0	
		10	3.3	1.6	3.2	
		50	3.3	2.75	3.0	
		50	33	1.30	3.2	
benzo[<i>h</i>]quinoline	-2.12	2	3.3	4.4	5.4	5.2
		20	3.3	22.1	5.2	
		2	33	2.2	5.3	
		20	33	7.6	5.2	
methyl benzoate	-2.17	2	3.3	4.3	5.4	5.5
		2	33	2.9	5.7	
chrysene	-2.20	1	0.033	$\delta E_p = 100$ mV	6.0	6.0

Table VII. Redox Catalysis of 3-Chloropyridine Reduction

catalyst	E^0_{PQ} , V vs. SCE	typical values of γ and v , V s ⁻¹		$(i_p)_c/(i_p)_0$	$\log k_1$, M ⁻¹ L s ⁻¹	av
9,10-diphenyl- anthracene	-1.80	20	0.033	1.10	0.2	1.0
		50	0.033	1.20	0.0	
anthracene	-1.89	2	0.033	1.26	1.6	1.5
		20	0.033	2.8	1.4	
		20	0.33	1.32	1.6	
phenanthridine	-2.00	1	0.33	1.76	3.4	3.5
		20	0.33	7.4	3.4	
		2	3.3	1.30	3.6	
		20	3.3	3.30	3.6	
		50	33	1.80	3.6	
benzo[<i>f</i>]quinoline	-2.08	1	3.3	1.73	4.4	4.5
		2	3.3	2.44	4.6	
		2	33	1.32	4.6	
benzo[<i>h</i>]quinoline	-2.12	2	3.3	4.33	5.4	5.5
		1	33	1.87	5.5	
		2	33	2.70	5.6	
methyl benzoate	-2.17	1	0.033	$\delta E_p = 105$ mV	6.1	6.1

transfer

$$\log k_1 = \log k_S^{\text{sol}} - \alpha^{\text{sol}}(E^0_{PQ} - E^0)/0.058 \quad (18)$$

with a homogeneous transfer coefficient $\alpha^{\text{sol}} = 0.5$ for the straight line with the $-1/116$ mV slope; (2) diffusion control

$$\log k_1 = \log k_{\text{dif}} - (E^0_{PQ} - E^0)/0.058 \quad (19)$$

for the straight line with the $-1/58$ mV slope.

Anion Radical as an Actual Reaction Intermediate vs. Simultaneous Electron Transfer and Breaking of the Carbon-Halogen Bond. The above interpretation assumes that the first electron transfer and the decomposition of the anion radical are two actually different successive steps. The observation in the $\log k_1 - E^0_{PQ}$ plot of a linear portion with a $-1/58$ mV slope provides therefore evidence that the anion radical is an actual intermediate in the reductive cleavage of halobenzenes and halopyridines. In the case of iodobenzene, where the above determinations were not carried out, the same conclusion also seems to hold. Indeed, if it is assumed that the reduction is under the combined kinetic control of electron transfer and a follow-up chemical reaction, it follows immediately that the anion radical is an actual reaction intermediate. On the other

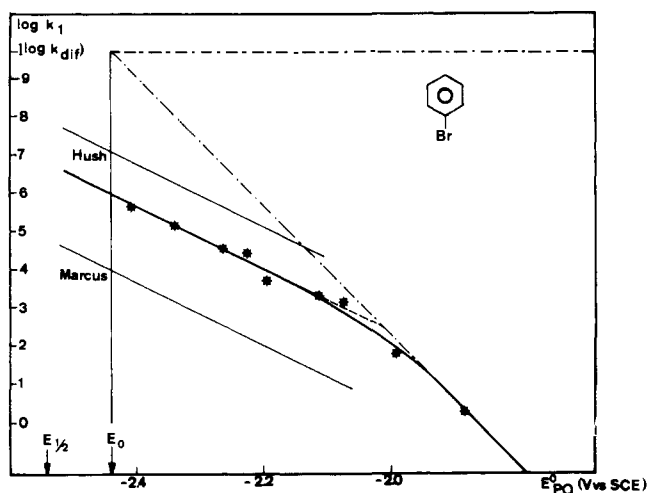
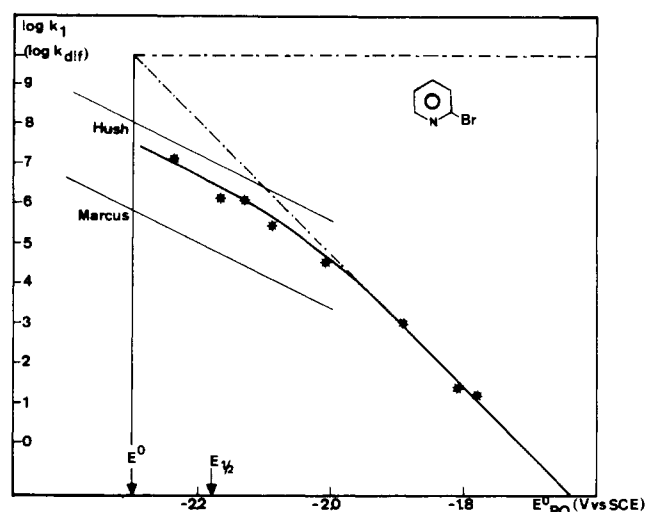
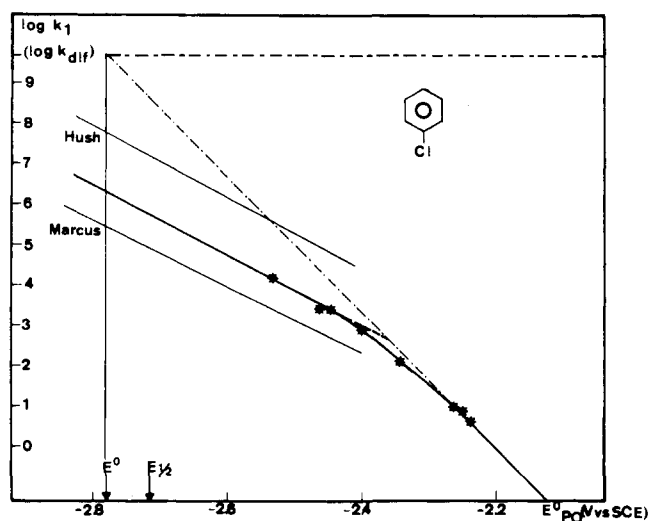
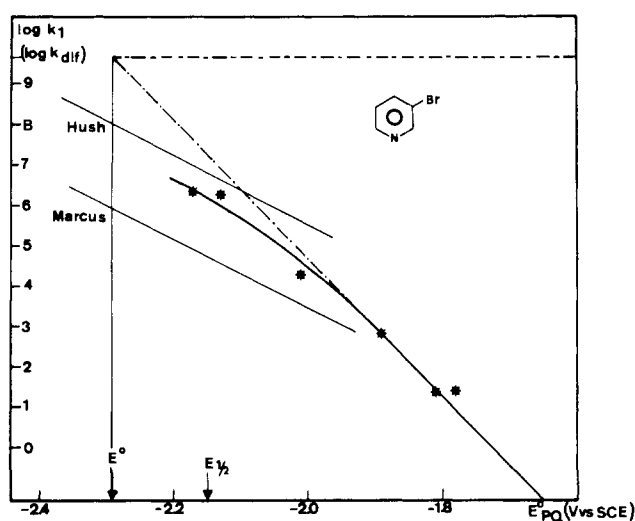
hand, under the assumption of a rate-determining charge transfer, the observation of a transfer coefficient significantly larger than 0.5 is inconsistent with a simultaneous electron transfer and bond-breaking reaction. Under such conditions indeed, the actual reduction potential would be negative to the standard potential of the overall reaction $\text{PhI} + 1e \rightleftharpoons \text{Ph}\cdot + \text{I}^-$, which would lead to an α smaller than 0.5. The opposite assumption of the anion radical being an actual reaction intermediate is on the contrary compatible with $\alpha > 0.5$ provided that the charge transfer and the chemical reaction are fast.¹⁹ These results are in agreement with the conclusion of a radiolysis study¹³ as regards PhCl and PhBr but contrast with those of PhI. It must, however, be borne in mind that the environmental conditions are largely different: homogeneous electron transfer in nonpolar medium for the radiolysis study, electrode transfer in polar solvent with a large concentration of an electrolyte in our case.

Standard Potentials and Standard Rate Constants of the ArX/ArX^{-•} Systems. According to eq 19 $E^0_{AB} = E^0_{PQ}$ when $(\log k_1)^{\text{dif}} = \log k_{\text{dif}}$. k_{dif} is not very different from one compound to the other as for the diffusion coefficients discussed above. It can be estimated as 5×10^9 M⁻¹ L s⁻¹.¹⁶

This allows the determination of the standard potential of

Table VIII. Reduction of Halobenzenes and Halopyridines. Heterogeneous Electron Transfer Characteristics. Predicted (Hush, Marcus) Homogeneous Characteristics

compd		PhBr	PhCl	2-pyBr	3-pyBr	2-pyCl	3-pyCl
E^0 , V vs. SCE		-2.44	-2.78	-2.30	-2.29	-2.40	-2.39
$k_S^{cl,ap}$, $cm\ s^{-1}$		2.4×10^{-4}	6.3×10^{-3}	2.0×10^{-2}	2.9×10^{-2}	4.4×10^{-2}	6.5×10^{-2}
$-\phi_2$, mV		136	142	132	130	134	134
k_S^{cl} , $cm\ s^{-1}$		3.6×10^{-3}	1.1×10^{-1}	2.7×10^{-1}	3.9×10^{-1}	6.2×10^{-1}	8.9×10^{-1}
$\Delta G_{cl}^*/F$, V		0.36	0.27	0.25	0.24	0.23	0.22
$\Delta G_{ArX}^{*iso}/F$, V	Hush	0.36	0.27	0.25	0.24	0.23	0.22
	Marcus	0.71	0.545	0.50	0.48	0.455	0.44
$\Delta G_{sol}^*/F$, V	Hush	0.26	0.215	0.205	0.20	0.19	0.19
	Marcus	0.44	0.35	0.33	0.32	0.31	0.30
k_S^{sol} , $M^{-1}\ L\ s^{-1}$	Hush	1.1×10^7	6.1×10^7	1.0×10^8	1.1×10^8	1.6×10^8	1.7×10^8
	Marcus	9.3×10^3	2.7×10^5	7.9×10^5	1.1×10^6	1.6×10^6	2.5×10^6

**Figure 3.** Bromobenzene. Homogeneous forward electron transfer rate constant, k_1 , vs. standard potential of the catalyst, E^0_{PQ} .**Figure 5.** 2-Bromopyridine. Homogeneous forward electron transfer rate constant, k_1 , vs. standard potential of the catalyst, E^0_{PQ} .**Figure 4.** Chlorobenzene. Homogeneous forward electron transfer rate constant, k_1 , vs. standard potential of the catalyst, E^0_{PQ} .**Figure 6.** 3-Bromopyridine. Homogeneous forward electron transfer rate constant, k_1 , vs. standard potential of the catalyst, E^0_{PQ} .

each halo compound/anion radical couple along a procedure pictured in Figures 3–8. The values of the polarographic $E_{1/2}$, for a 2-s drop time, are also indicated in Figures 2–8, for rapid comparison with the E^0 's. From the values of E^0_{AB} (first row in Table VIII) and from those of the heterogeneous forward electron transfer rate constant previously determined (last row of Table I) it is now possible to evaluate the apparent standard rate constant of the electrode electron transfer, $k_S^{cl,ap}$. The results of this evaluation are given in Table VIII. No such determination is possible in the case of iodobenzene. It can,

however, be stated that the standard rate constant is larger than for chloro- and bromobenzene. In order to prove this, let us consider successively the two assumptions regarding the rate-determining step as discussed above. In the case of a mixed kinetic control by charge transfer and follow-up reaction, the fact that I^- is a better leaving group than both Cl^- and Br^- implies that the follow-up reaction is faster in the former case than in the latter cases. Since charge transfer is rate determining with PhCl and PhBr, this means that charge transfer has to be faster with PhI in order not to have become rate de-

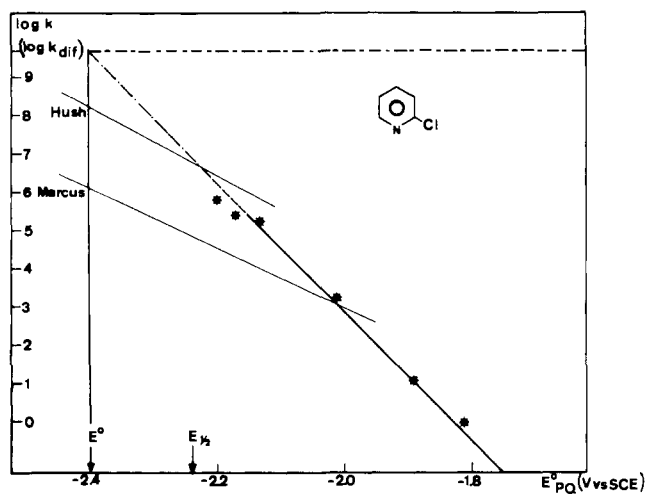


Figure 7. 2-Chloropyridine. Homogeneous forward electron transfer rate constant, k_1 , vs. standard potential of the catalyst, E°_{PQ} .

termining. This conclusion also matches the observation that catalytic efficiency is smaller with PhI than with PhCl and PhBr as expected for a mixed kinetically controlled system.¹¹ In the case, now, of a rate-determining charge transfer the low catalytic efficiency obtained with PhI provides again evidence that charge transfer is faster than with PhCl and PhBr. Also the fact that α would be significantly larger than 0.5 indicates that the actual potential is markedly positive to the standard potential, more than with PhCl and PhBr, which again means that the charge transfer standard rate is larger.

Correlation between Homogeneous and Heterogeneous Electron Transfer Kinetics. The homogeneous standard rate constant is expected to increase with $k_S^{cl,ap}$. This explains why the linear portion with a $-1/58$ mV slope extends on a larger and larger region at the expense of the second linear portion when passing from bromobenzene to 3-chloropyridine, i.e., when the charge transfer becomes faster and faster (compare Figures 3–8 with the $k_S^{cl,ap}$ values listed in Table VIII).

It is also possible to carry out a more detailed comparison of the homogeneous and heterogeneous electron transfer kinetics. For this, let us compare the experimental data for the homogeneous process in the activation region (left part of the $\log k_1 - E^{\circ}_{PQ}$ plots) to the values predicted by the Hush^{20,21} or Marcus^{22,23} theoretical relationships between homogeneous and heterogeneous electron transfer kinetics starting from the experimental data for the heterogeneous process.

k_S^{cl} is first derived from $k_S^{cl,ap}$ carrying out a Frumkin correction on the basis of the OHP potentials ϕ_2 , previously determined in DMF with 0.1 M Bu_4NI .²⁴

The electrochemical activation free energy ΔG^*_{cl} is then obtained from eq 17 taking $Z^{cl} \approx 5 \times 10^3$ cm s⁻¹.¹⁶ A predicted value of the homogeneous isotopic activation free energy of the ArX/ArX^- couple can then be evaluated, either as $\Delta G^*_{ArX^{iso}} = \Delta G^*_{cl}$ (Hush theory) or as $\Delta G^*_{ArX^{iso}} = 2\Delta G^*_{cl}$ (Marcus theory). The predicted value of the cross-exchange free energy is then obtained from eq 14 and that of the cross-exchange standard rate constant from eq 13 taking $Z^{sol} = 3 \times 10^{11}$ M⁻¹ L s⁻¹.

The results of these evaluations are given in Table III. On these bases, two straight lines corresponding respectively to Hush and Marcus predictions in the activation region have been drawn on the $\log k_1 - E^{\circ}_{PQ}$ plots (Figures 3–8). It is seen that the experimental points fall in the region comprised between the Hush and Marcus lines. One may also notice that there is a rough tendency of passing from the Marcus to the Hush behavior as the electron transfer becomes faster and faster. Note in this connection that for faster charge transfers

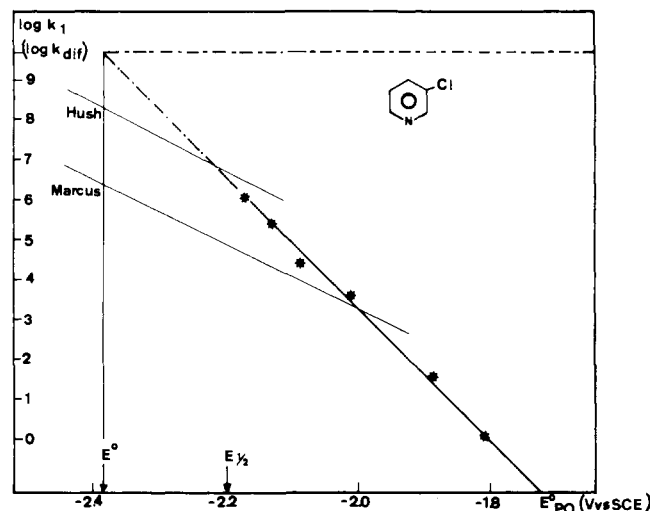


Figure 8. 3-Chloropyridine. Homogeneous forward electron transfer rate constant, k_1 , vs. standard potential of the catalyst, E°_{PQ} .

without accompanying chemical reactions the Hush behavior is mostly observed.¹⁶

Relationships between ArX Structure and the Standard Potentials. A first observation is that the standard potentials are more positive for the bromo than for the chloro derivatives in both series. One also notes that the effect is much more pronounced in the benzene series (340 mV) than in the pyridine series (100 mV). It is interesting to compare these observations with what happens with other halo aromatics or heteroaromatics. There are in fact relatively few cases where reliable E° values unaffected by either charge-transfer kinetics or by follow-up reactions are available. They concern compounds involving facile accommodation of a negative charge on the ring (phenazine²⁵) or on a conjugative electron-withdrawing substituent ($-COR$,^{26,27} NO_2 ^{28,29}), hence giving rise to stable anion radicals and to fast electron transfers. A general picture, however, emerges from this comparison (Table IX): (1) the E° 's of the bromo derivatives are constantly more positive than those of the chloro derivatives; (2) the difference between Br and Cl decreases considerably from benzene to good electron-accepting rings. Note in this connection that pyridine is a better electron-accepting ring than benzene due to the imine-like character of the CN bond.³⁰ These observations can be rationalized as follows.

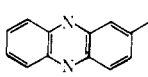
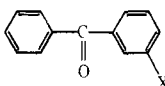
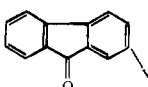
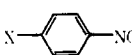
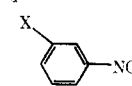
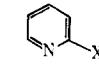
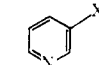
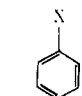
(1) With the strongly electron-accepting rings the largest part of the negative charge in the anion radical lies on the ring or on the activating group rather than on the halogen atom, the influence of which can therefore be thought as an inductive-conjugative perturbation of the π LUMO. The difference between Cl and Br derivatives may then be rationalized in terms of σ -Hammett constants²⁶ and is therefore predicted to be small.³¹

(2) In the case of halobenzenes, the lowest unoccupied orbital is likely to be the σ LUMO rather than the π LUMO and a large part of the charge in the anion radical located on the halogen atom.³² It is anticipated in these conditions that Br will accommodate more negative charge than Cl in accordance with Br^- being a better leaving group than Cl^- .

(3) Pyridine is expected to correspond to an intermediate situation, the electron-accepting character of the ring being certainly larger than in benzene but weaker than in phenazine, nitrobenzene, and aromatic ketones.

(4) It follows that electron affinity will be larger for Br than for Cl derivatives and that the difference between them will decrease as, in the anion radical, the ring or the other electron-withdrawing substituents are able to accommodate more

Table IX. Standard Potential Difference between Bromo and Chloro Aromatics and Heteroaromatics

compd	$E^0_{ArBr} - E^0_{ArCl}$, mV	solvent	ref
 (2-halophenazine)	10	DMF	25
 (<i>m</i> -halobenzophenone)	20	liq NH ₃ (-40 °C)	27
 (2-halofluorenone)	25	DMF	26
 (<i>p</i> -halonitrobenzene)	30	MeCN	28
 (<i>m</i> -halonitrobenzene)	40	MeCN	28
 (2-halopyridine)	100	DMF	this work
 (3-halopyridine)	100	DMF	this work
 (halobenzene)	340	DMF	this work

and more negative charge. These are indeed the trends followed by the standard potentials.

(5) It must, however, be examined if the solvation effects which also influence the E^0 's may reverse the variations predicted on the basis of electron affinity. Solvation effects on the standard potentials essentially involve the anion radical and can be roughly described in terms of a two-sphere Born model (Figure 9) as already used for representing the solvent reorganization factor in electron transfer kinetic studies of nitro compounds.³³ Assuming that $\frac{2}{3}$ of the negative charge is located on the Cl atom in PhCl,³⁴ the maximum of the solvation effect in favor of a better reducibility for PhCl than for PhBr would be 130 mV, corresponding to equal fractional charges on Cl and Br. The effect of solvation becomes zero for a fractional charge of 0.7 on Br as compared with 0.66 for Cl. The difference in fractional charges is in fact probably larger, which results in the solvation effect being in the same direction as the electron affinity effect. Similar conclusions will also hold for pyridine. For the other molecules the solvation effect is predicted to be extremely small, the major part of the charge being located on the ring or on the other substituent.

(6) The preceding analysis not only explains the observed variations of $E^0_{ArBr} - E^0_{ArCl}$ with structure but also the fact that $E^0_{pyBr} - E^0_{PhBr} < E^0_{pyCl} - E^0_{PhCl}$ (Table VIII): more negative charge being located on the Br atom than on the Cl atom, the E^0 's are less sensitive to variations of the electron-accepting character of the ring in the first case than in the second.

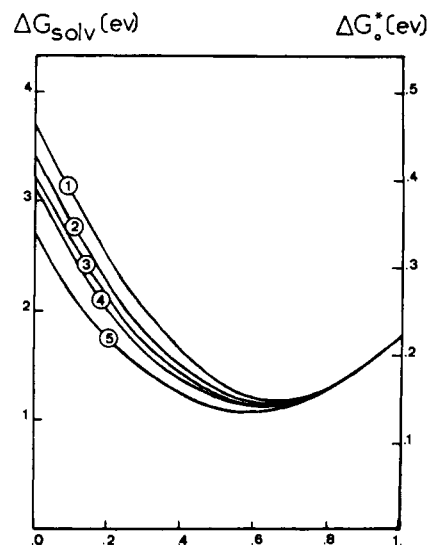


Figure 9. Two-sphere Born model. Variations of the solvation energy (ΔG_{solv}) and of the solvent reorganization activation energy (ΔG_0^*) with the fractional charge (q) on the ring for benzene and pyridine derivatives: (1) Cl, (2) Br, (3) CN, (4) I, (5) NO₂. Radii (Å): Ph and py, 3.68; Cl, 1.80; Br, 1.95; CN, 2.08; I, 2.15; NO₂, 2.5.

Electron-Transfer Kinetics and Structure. $k_S^{el,ap}$ can be used without difficulty comparing the electron transfer kinetic characteristics of the halobenzene and halopyridines since the potentials at the OHP are nearly the same for all compounds (Table VIII). The following trends are immediately apparent: (1) Electron transfer is much slower for bromo- and chlorobenzene and pyridine than for other aromatic compounds such as nitrobenzene, benzonitrile, and cyanopyridine¹⁶ (standard rate constant are lower by one to four orders of magnitude). (2) Rate constants are markedly lower in the benzene series than in the pyridine series. (3) Bromo derivatives give rise to slower electron transfer than chloro derivatives and this trend is more significant for benzene than for pyridine. (4) Electron transfer to iodobenzene is faster than in the case of bromo- and even chlorobenzene as discussed previously.

In the context of Hush theory, the part of the activation energy dealing with solvent reorganization can be expressed as

$$\Delta G_0^* = e^2/8[q^2/R_{ring} + (1-q)^2/R_{sub}][(1/D_{op}) - (1/D_S)] - (e^2/16)(1/\delta)[(1/D_{op}) - (1/D_S)]$$

according to a two-sphere Born model of solvation³³ (q = fractional charge on the ring; R_{ring} , R_{sub} = ring and substituent radius, respectively; δ = distance between electrode and reaction site; $D_{op} = 2.04$, $D_S = 36.7$ for DMF, D_S and D_{op} being the static dielectric constant and the optical dielectric constant, respectively. The second term, which is about the same for each compound, can be evaluated in two ways. In the first, δ is assumed to be very large, which amounts to neglecting the double-layer correction, thus considering that $k_S^{el,ap} = k_S^{el}$ and computing ΔG^* directly from the $k_S^{el,ap}$. In the second, ϕ_2 is taken as equal to -130 to -140 mV and the second term in ΔG^* appears as equivalent to the Frumkin correction when $\delta \approx 6$ Å, which is a satisfactory estimation for the distance between the OHP and the electrode with tetrabutylammonium as supporting cation. It follows that, in both cases, estimation of ΔG_0^* can be carried out directly from the $k_S^{el,ap}$ neglecting the second term. The values of ΔG_0^* calculated from the first term are represented in Figure 9 as a function of the fractional charge for PhCl, PhBr, PhI, PhCN, and PhNO₂. On the other hand, the ΔG^* (eV) computed from the experimental $k_S^{el,ap}$ are the following: PhBr, 0.44; PhCl, 0.35; PhI, <0.35; 2-pyBr, 0.32; 3-pyBr, 0.31; 2-pyCl, 0.30; 3-pyCl, 0.29; PhCN, 0.24;

PhNO₂, 0.20. It is seen by comparison with the diagrams of Figure 8 that for the halobenzenes and halopyridines the identification of the experimental ΔG^* to the ΔG_0^* would imply the localization of a very high charge density on the halogen atom whereas more reasonable values are obtained with PhCN and PhNO₂. In the case of PhBr, the fractional charge on Br would even be larger than 1, clearly showing that solvent reorganization is not the only significant factor determining the magnitude of the electron-transfer rate. Note also that Born models of solvation energy generally result in overestimation especially for small radii and that Marcus theory would predict smaller ΔG_0^* , which reinforces the above conclusion.

One must therefore conclude that internal reorganization, i.e., charge in bond lengths and angles between the starting molecule and its anion radical, plays a significant role in determining the kinetics of electron transfer to halobenzenes and halopyridines. Indeed, in accordance with the strong tendency for the halogen to cleave off after the first electron uptake, it is very likely that stretching of the carbon-halogen bond is quite significant when passing from the starting molecule to the anion radical. This is related to the dominance of the σ character of the electron-accepting orbital in the halo compounds in contrast with conjugative electron-withdrawing groups such as CN and NO₂ for which the anion radicals are indeed quite stable and the changes in bond lengths and angles are small as in all cases where the π -electron system is delocalized over the entire molecule.³⁴

Under these conditions, the experimental variations of electron-transfer kinetics with structure, as underlined above, can be interpreted as resulting from the following effects on solvent and internal reorganization factors: (1) Solvation reorganization energy increases slightly from Cl to Br and then decreases from Br to I. For the same halogen it is larger for benzene than for pyridine since the fractional charge on the ring is smaller in the first case than in the second. (2) Internal reorganization energy increases in the series Cl < Br < I together with the leaving-group ability, this effect being, however, moderated by the increase of the back-bonding when passing from Cl to I. Internal reorganization is expected to be smaller with pyridine than with benzene since less negative charge is located on the halogen in the first case than in the second.

Acknowledgment. The work was supported in part by the CNRS (Equipe de Recherche Associée 309 "Electrochimie

Moléculaire"; ATP CNRS-EDF "Utilisations Physiques et Chimiques de l'Electricité").

References and Notes

- (1) F. M'Halla, J. Pinson, and J. M. Saveant, *J. Electroanal. Chem.*, **89**, 347 (1978).
- (2) J. Pinson and J. M. Savéant, *J. Am. Chem. Soc.*, **100**, 1506 (1978).
- (3) S. O. Farwell, F. A. Beland, and R. D. Geer, *J. Electroanal. Chem.*, **61**, 303 (1975).
- (4) S. O. Farwell, F. A. Beland, and R. D. Geer, *J. Electroanal. Chem.*, **61**, 315 (1975).
- (5) R. N. Renaud, *Can. J. Chem.*, **52**, 376 (1974).
- (6) D. E. Bartak, K. J. Houser, B. C. Rudy, and M. D. Hawley, *J. Am. Chem. Soc.*, **94**, 7526 (1972).
- (7) C. Amatore, J. Chaussard, F. M'Halla, J. Pinson, J. M. Savéant, and A. Thiébaud, unpublished results.
- (8) L. Nadjo and J. M. Savéant, *J. Electroanal. Chem.*, **48**, 113 (1973).
- (9) C. P. Andrieux, J. M. Dumas-Bouchiat, and J. M. Savéant, *J. Electroanal. Chem.*, **87**, 55 (1978).
- (10) C. P. Andrieux, J. M. Dumas-Bouchiat, and J. M. Saveant, *J. Electroanal. Chem.*, **87**, 39 (1978).
- (11) C. P. Andrieux, J. M. Dumas-Bouchiat, and J. M. Savéant, in course of publication.
- (12) W. E. Wentworth, R. George, and H. Keith, *J. Chem. Phys.*, **51**, 1791 (1969).
- (13) J. C. Steelhammer and W. E. Wentworth, *J. Chem. Phys.*, **51**, 1802 (1969).
- (14) S. Bank and D. A. Juckett, *J. Am. Chem. Soc.*, **98**, 7742 (1976).
- (15) R. Marcus in "Dahlem Workshop on the Nature of Sea Water", Dahlem Konferenzen, E. D. Goldbery, Ed., Abakou, Berlin, 1975, pp 478-504.
- (16) H. Kojima and A. J. Bard, *J. Am. Chem. Soc.*, **97**, 6317 (1975).
- (17) H. Matsuda and Y. Ayabe, *Z. Elektrochem.*, **59**, 494 (1955).
- (18) A. J. Fry, C. S. Hutchins, and L. L. Chung, *J. Am. Chem. Soc.*, **97**, 591 (1975).
- (19) J. M. Savéant and D. Tessier, *J. Phys. Chem.*, **82**, 1723 (1978).
- (20) N. S. Hush, *J. Chem. Phys.*, **28**, 962 (1958).
- (21) N. S. Hush, *Trans. Faraday Soc.*, **57**, 557 (1961).
- (22) R. A. Marcus, *J. Chem. Phys.*, **24**, 4966 (1956).
- (23) R. A. Marcus, *J. Chem. Phys.*, **43**, 679 (1965).
- (24) J. M. Savéant and D. Tessier, *J. Phys. Chem.*, **81**, 2192 (1977).
- (25) K. Alwair and J. Grimshaw, *J. Chem. Soc., Perkin Trans. 2*, 1811 (1973).
- (26) L. Nadjo and J. M. Savéant, *J. Electroanal. Chem.*, **30**, 41 (1971).
- (27) J. M. Savéant and A. Thiébaud, *J. Electroanal. Chem.*, **89**, 335 (1978).
- (28) R. F. Nelson, A. K. Carpenter, and E. T. Seo, *J. Electrochem. Soc.*, **120**, 206 (1973).
- (29) J. G. Lawless and M. D. Hawley, *J. Electroanal. Chem.*, **21**, 365 (1969).
- (30) This is essentially why pyridine itself is easier to reduce than benzene (in DMF the E^0 for pyridine is about -2.6 V vs. SCE whereas no reduction wave for benzene can be seen before the discharge of the supporting electrolyte).
- (31) P. Zuman, "Substituent Effects in Organic Polarography", Plenum Press, New York, 1967.
- (32) F. A. Beland, S. O. Farwell, P. R. Callis, and R. D. Geer, *J. Electroanal. Chem.*, **78**, 145 (1977).
- (33) M. E. Peover and J. S. Powell, *J. Electroanal. Chem.*, **20**, 427 (1969).
- (34) J. M. Hale, "Reactions of Molecules at Electrodes", N. S. Hush, Ed., Wiley-Interscience, New York, 1971, Chapter 4.